Oxidation of di-n-propyl ether: Characterization of low-temperature products

Nesrine Belhadj, Roland Benoit, Philippe Dagaut, Maxence Lailliau, Zeynep Serinyel, Guillaume Dayma

Oxidation of di-n-propyl ether: characterization of low-temperature products

Nesrine Belhadj[1,2], Roland Benoit[1], Philippe Dagaut[1,*], Maxence Lailliau[1], Zeynep Serinyel[1,2], Guillaume Dayma[1,2]

[1] CNRS–INSIS, CARE, 1C avenue de la Recherche Scientifique, 45071 Orléans cedex 2, France

[2] Université d'Orléans, rue de Chartres, 45100 Orléans, France

Abstract

The oxidation of di-n-propyl-ether (DPE) was performed in a jet-stirred reactor at 1 and 10 atm, at residence times of 1 and 0.7 s, respectively, and initial fuel concentrations of 5000 and 1000 ppm at 1 and 10 atm, respectively. Atmospheric pressure experiments were used for characterization of cool flame products. The 10 atm experiment provided KHPs profile vs. temperature and mole fraction profiles of stable species which were obtained through sonic probe sampling, gas chromatography, Fourier transform infrared spectrometry analyses. High resolution mass spectrometry analyses (HRMS) with syringe direct injection or ultra-high-pressure liquid chromatography coupling was used to characterize hydroperoxides ($C_3H_8O_2$, $C_6H_{14}O_3$), diols ($C_6H_{14}O_3$), ketohydroperoxides ($C_6H_{12}O_4$), carboxylic acids, and highly oxygenated molecules ($C_6H_{12}O_6$, $C_6H_{12}O_8$) resulting from up to four O_2 additions on fuel's radicals. Heated electrospray and atmospheric pressure chemical ionizations (HESI and APCI) were used in positive and negative mode. Whereas the CH_2 groups neighboring the ether function are the most favorable sites for H-atom abstraction reactions, speciation indicated that other sites can react by metathesis forming a large pool of intermediates. Our kinetic reaction mechanism represents the experimental data for most of the stable species but need to be expended for simulating the formation of newly detected species.

Keywords: dipropyl ether, jet-stirred reactor, cool flame, ketohydroperoxides, highly oxygenated molecules

Introduction

In the recent years, the interest for alternative biofuels has been growing. Ethers, which can be synthesized via dehydration of alcohols, are among the chemicals of interest. Very recently, the kinetics of oxidation of di-n-butyl ether and diethyl ether received much attention [1-9]. For di-n-propyl ether (CAS 111-43-3), only one chemical kinetic study has been reported [10] whereas it easily oxidizes at low temperature, making it a good candidate for further investigating the formation of ketohydroperoxides [11-19], and recently proposed new oxidation pathways [20, 21] leading to highly oxygenated molecules (HOMs). Whereas HOMs are minor combustion products, in the troposphere they are considered of paramount importance for the formation of secondary organic aerosols [22]. In previous studies, chromatographic separation of ketohydroperoxides, formed by oxidation of large hydrocarbons, and detection by UV absorption or mass spectrometry was attempted [11-19], but suffered from instruments limitations. With more powerful techniques such as ultra-high-pressure liquid chromatography and Orbitrap ® mass spectrometry, one can expect improving the characterization of low temperature oxidation products. This was initiated in our preliminary investigation [23]. Here, new experiments were performed in a JSR to characterize the DPE low temperature oxidation products. Hydroperoxides, ketohydroperoxides, carboxylic acids, cyclic ethers, highly oxygenated molecules resulting from multiple O_2 addition were tracked using soft chemical ionization and high-resolution mass spectrometry. After having verified that our chemical kinetic model for the oxidation of di-n-propyl ether (DPE) [10] could represent experimental results obtained for stable products, we used it to simulate the global formation of ketohydroperoxides.

Experimental

Experiments were performed in a fused silica jet-stirred reactor (JSR) setup already described in details [24] and used in previous studies [25-27]. As in previous works [9, 25] the liquid fuel (>98% pure from TCI) was atomized by a nitrogen flow and vaporized in a heated chamber. The fuel and oxygen were sent separately to the JSR to avoid oxidation before reaching the 4 injectors (nozzles of 1 mm I.D.) providing stirring. Flow rates of the nitrogen diluent and oxygen were controlled by mass flow meters. The liquid fuel was pumped using an HPLC pump (Shimadzu LC10 AD VP) with an online degasser (Shimadzu DGU-20 A3). Good thermal homogeneity along the vertical axis of the JSR was recorded (gradients of < 1 K/cm) by thermocouple measurements (0.1 mm Pt-Pt/Rh-10% wires located inside a thin-wall silica tube). A low-pressure sonic probe was used to freeze the reactions and take samples for online and off line analyses. The samples were sent to analyzers via a Teflon heated line (200 °C). Online Fourier transform infrared (FTIR) spectrometry (10m path length, 200 mBar, resolution of 0.5 cm^{-1}) was used to measure water, carbon monoxide, carbon dioxide, formaldehyde, and propionic acid. As earlier [9, 25], off line analyses by gas chromatography (GC) with flame ionization and thermal conductivity detection were used for the measurement of stable species (di-n-propyl-ether, O_2, H_2, CO, CO_2, C_2H_4, CH_4, C_2H_6, C_3H_6, formaldehyde, propanal, acetaldehyde, and propanoic acid). Quantifications were performed using external standards. Several

other minor oxygenated species were also identified (maximum concentration in the cool flame in parentheses), such as 1-propanol (5 ppm), cis- and trans-2-ethyl-4-methyl-1,3-dioxolane (60 ppm), 2-(propoxymethyl) oxirane (4 ppm), propyl formate, (9 ppm) and ethyl formate (5 ppm). Capillary columns (DB-624, CP-Sil5CB, CP-Al_2O_3-KCl, and Carboplot-P7) where used for GC analyses.

To measure hydroperoxides, ketohydroperoxides (KHPs) and other low temperature oxidation products, the sonic probe samples were bubbled into cooled acetonitrile (-15°C, 250 mL for 1 atm experiments and 25 mL for others) for 90 min. The resulting solutions were stored in a freezer at -30°C. Compared to direct gas sample injection, this procedure allows performing many analyses with a single sample, which is useful for optimizing the analytical conditions. Analyses were performed by direct sample instillation (flow injection of 3µL/mn recorded for 1 min for data averaging) in the ionization chamber of an Orbitrap ® Q-Exactive Mass spectrometer (mass resolution of 140,000 and mass accuracy <0.5 ppm RMS). Mass calibrations were performed weekly using Pierce ESI positive ion calibration solution and Pierce ESI negative ion calibration solution Refs. 88323 and 88324 (Thermo Scientific), respectively.

Ultra-high pressure liquid chromatography (UHPLC) analyses were performed using an analytical column (C_{18} Phenomenex Luna, 1.6µm, 100 Å, 100x2.1 mm) for products separation after injection of 3 µL of sample eluted by water-acetonitrile (ACN) at a flow rate of 250 µL/min (gradient 5% to 85% ACN). Ion Max heated electrospray ionization (HESI) and atmospheric chemical ionization (APCI) were used in positive and negative modes for the ionization of products. APCI settings were: vaporizer temperature of 150°C, sheath gas flow of 55 a.u., auxiliary gas plow of 6 a.u., sweep gas flow of 0 a.u., capillary temperature of 300°C, corona current of 3µA. In HESI mode, we used a spray voltage of 3.8 kV. Oxidation of analytes by HESI has been reported previously [28, 29]. In the present study, we verified that no oxidation occurred in the ion source by injecting a DPE-ACN solution in both HESI and APCI.

To determine the structure of cool flame products, MS-MS analyses were performed at collision cell energy of 10 eV. The fast OH/OD exchange [21] was employed to verify the presence of hydroxyl and hydroperoxy groups in the products. To this end, we added 300 µL of D_2O (Sigma-Aldrich) to 1.5 mL of sample. The resulting solution was analyzed by flow injection and APCI mass spectrometry. The carbon balance was checked for each sample; it was found to be typically within ±10–15%.

Kinetic modeling

The computations were performed using the PSR computer code [30] from the Chemkin II package[31]. Our kinetic mechanism presented earlier [10] and consisting of 528 species and 3062 reactions was used. Our mechanism includes both low- and high-temperature chemistry but is limited to 2 additions of O_2 to fuel's radicals which yield ketohydroperoxides. The formation of the most likely KHPs at 510 K during the oxidation of 1000 ppm of DPE at 10 atm is presented in Figure 1. According to our chemical kinetic modeling, DPE is mainly consumed through H-atom abstraction by hydroxyl radicals. The resulting fuel radicals get peroxided by reaction with molecular oxygen.

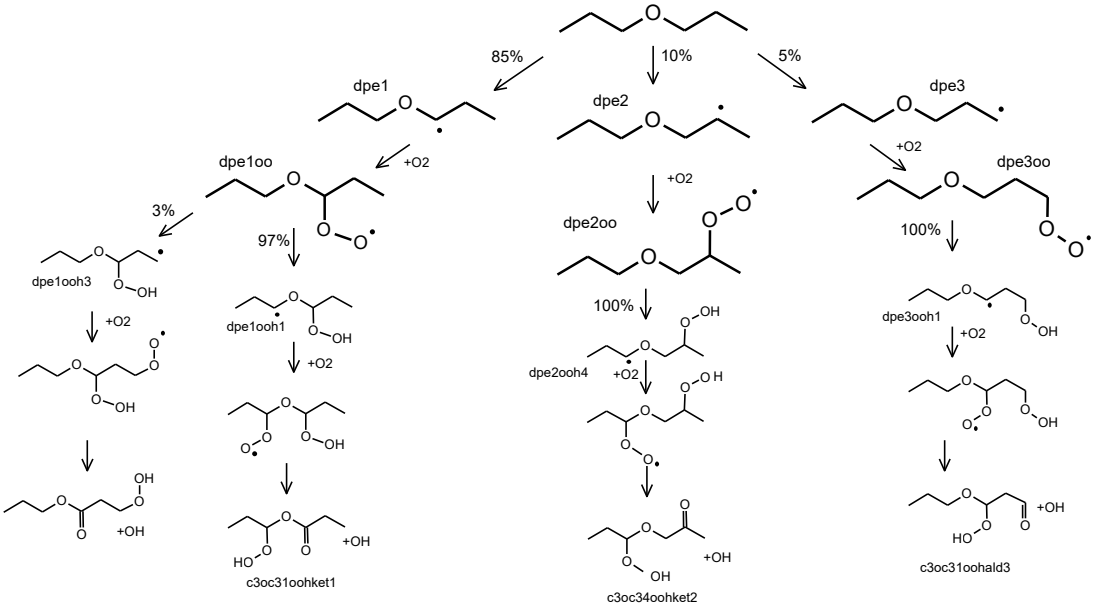

Figure 1. Formation of KHPs during the oxidation of DPE in fuel-lean conditions.

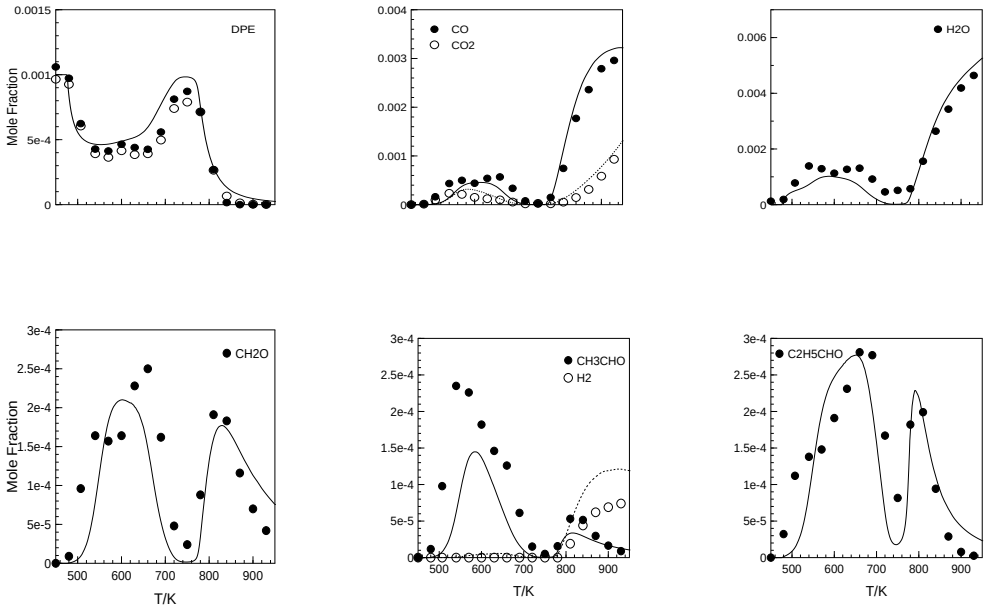

Figure 2. Mole fraction profiles (symbols: data, lines: computations) as a function of reactor temperature in K at φ = 0.5, 0.7 s, and 10 atm.

Figure 2 presents a comparison of experimental and computational results for selected stable species. Additional results are presented in Supplementary Material S1. Since the chemical kinetic model represents fairly well the data it was used to predict newly characterized species, namely ketohydroperoxides. The results are presented in the next section

Results and discussion

The formation of ketohydroperoxides and highly oxygenated compounds resulting from O_2 addition on the fuels radicals (R) was observed. Table 1 gives an overview of the results. More detailed information is provided in Supporting Material S2. Their formation proceeds through a sequence of reactions: R + O_2 ⇆ RO_2; RO_2 ⇆ QOOH; QOOH + O_2 ⇆ OOQOOH; OOQOOH ⇆ HOOQ'OOH followed by the formation of the hydroxyl radical and a ketohydroperoxide ($C_6H_{12}O_4$): HOOQ'OOH → HOOQ'O + OH. Dihydroperoxides can also react with molecular oxygen (3rd O_2 addition): HOOQ'OOH + O_2 ⇆ $(HOO)_2$Q'OO; $(HOO)_2$Q'OO ⇆ $(HOO)_2$POOH; $(HOO)_2$POOH → OH + $(HOO)_2$P=O ($C_6H_{12}O_6$). The reaction can also proceed through a 4th O_2 addition: $(HOO)_2$POOH + O_2 → $(HOO)_3$POO; $(HOO)_3$POO ⇆ $(HOO)_3$P'OOH; $(HOO)_3$P'OOH → OH + $(HOO)_3$P'=O ($C_6H_{12}O_8$). The products of third and fourth oxygen addition were observed in the present experiments confirming the extended oxidation pathways proposed earlier [21]. However, in a previous JSR study where we oxidized di-n-pentyl ether, only products of up to the third O_2 addition ($C_{10}H_{20}O_6$) could be observed by molecular beam-time of flight mass spectrometry and synchrotron photoionization [21]. Here, we also observed the formation of hydroperoxides ROOH (Table 1) which can result from H-atom abstraction by RO_2: RO_2 + R'H → ROOH + R'. Whereas $C_6H_{14}O_3$ hydroperoxides could be detected by presence of characteristic H_2O_2 loss in MS/MS [32], double H/D exchange also indicated the presence of diols with the same global formula (M-H+, m/z 135.1015). The Supporting Material S3 shows the UHPLC separation of $C_6H_{14}O_3$ isomers. The formation of diols was reported in previous work [16], and the authors indicated diols derive from di-hydroperoxides decomposition.

Table 1. Oxygenated species detected during the cool flame oxidation of di-n-propyl ether (5000 ppm of DPE, 1 atm, τ=1s, T=520 K, 90 min trapping in ACN.

Species	Ion formula	Ion m/z	OH/OD exchange
Propanoic acid	$C_3H_6O_2H^+$	75.0441	yes
Cyclic ethers	$C_6H_{12}O_2H^+$	117.0910	--
Propanoic anhydrid	$C_6H_{10}O_3H^+$	133.0859	--
Diols, hydroperoxides	$C_6H_{14}O_3H^+$	135.1015	yes
Ketohydroperoxides	$C_6H_{12}O_4H^+$	149.0808	yes
di-Ketohydroperoxides	$C_6H_9O_5^-$ $C_6H_{10}O_5Na^+$	165.0757 185.0426	yes
Keto- di -hydroperoxides	$C_6H_{11}O_6^-$ $C_6H_{12}O_6Na^+$ $C_6H_{12}O_6NH_4^+$	179.0555 203.0531 198.0977	yes yes yes[a]
HOMs	$C_6H_{11}O_8^-$	211.0454	yes

[a] sample dopped with 200 ppm of CH_3COONH_4

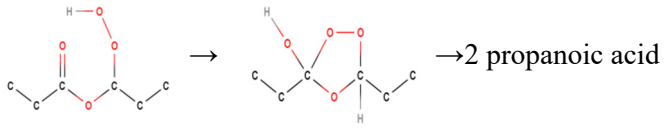

Figure 3. Formation of propanoic acid through the decomposition di-n-propyl ether ketohydroperoxide, according to the so-called Korcek mechanism.

The so-called Korcek mechanism [33], through which the ketohydroperoxides key-intermediates are transformed into stable products, namely propionic acid here (Fig. 3) can modify the overall system reactivity. Other channels could also contribute to the formation of propionic acid during DPE oxidation. Propionic acid was observed in the present experiments both in gas phase samples and liquid samples. As reported earlier [10], the present chemical kinetic model which includes the Korcek mechanism underestimated the mole fractions measured in the gas phase.

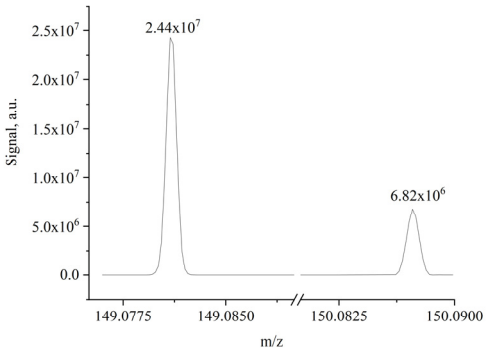

Figure 4. Mass spectrum showing the increased ratio $C_6H_{12}DO_4^+$/ $C_6H_{13}O_4^+$ due to OH/OD exchange on KHPs. Analyses were performed in APCI positive mode.

Hydrogen–Deuterium exchange reactions using D_2O were used to confirm the presence of –OH groups in the products (Table 1). An example of the observed H/D exchange for KHPs is given in Figure 4. One can see the increased ratio of $C_6H_{12}DO_4^+$/ $C_6H_{13}O_4^+$from 0 to 0.3. In absence of D_2O, no signal could be observed at m/z 150.0873, as expected based on the natural abundance of D, $1.5x10^{-4}$ [34], and the intensity of 2 $x10^7$ at m/z 149.0810, resulting in an intensity lower than detection limit (c.a. 3000) for deuterated KHPs.

Thanks to the use of UHPLC- HRMS-MS-MS with APCI we could separate and characterize the KHP isomers. Figure 5 presents a typical chromatogram obtained here, and the structure of KHPs is given in Table 2.

Table 2. Chemical structure of KHPs obtained by oxidation of DPE

Initial radicals formed by H-atom abstraction on the fuel		
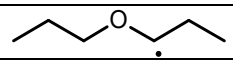	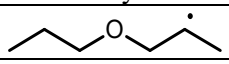	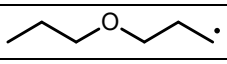
Deriving ketohydroperoxides, size of the cyclic intermediate during H-atom transfer and C-H bond type (p: primary, s: secondary), #: inverse order of dipole moment value given in parentheses (Debye)		
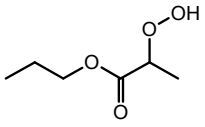 5,s ; #14 (1.42)	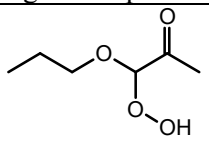 5,s ;#5 (4.86)	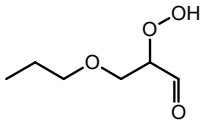 5,p ; #10 (3.58)
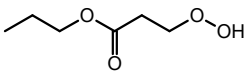 6,s ; #12 (1.68)	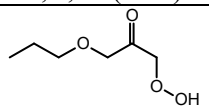 5,s ; #2(5.75)	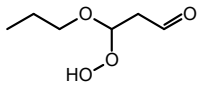 6,p ; #8 (3.86)
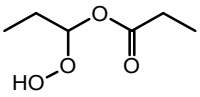 6,s ; #11 (2.32)*	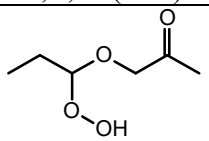 7,s ; #4 (4.90)	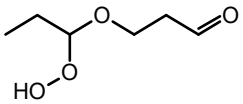 8,p ; #9 (3.83)
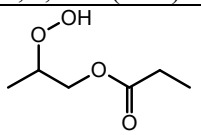 7,s ; #15 (1.38)	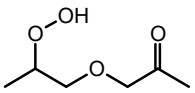 8,s ; #1 (5.82)	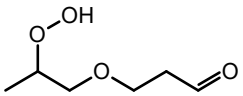 9,p ; #6 (4.54)
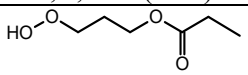 8,s ; #13 (1.52)	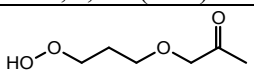 9,s ; #3 (5.72)	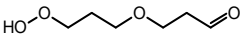 10,p ;#7 (3.90)

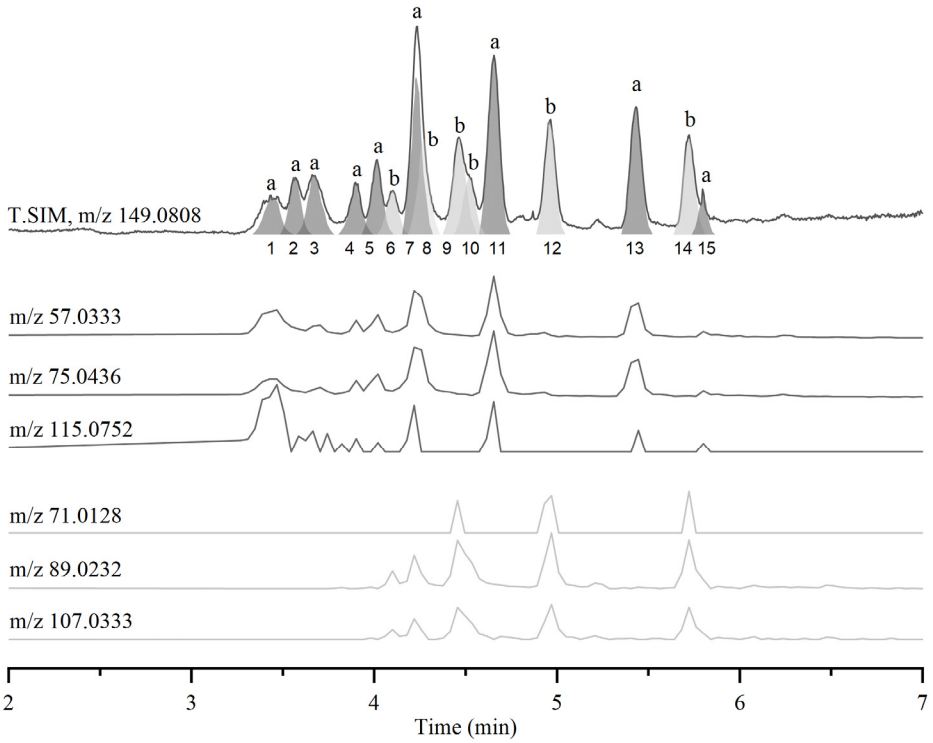

Figure 5. Typical chromatogram obtained for m/z 149.08084 (positive mode). KHPs with -OOH and -C=O on both sides of the ether function (a) and on one side (b) are indicated. Numbers refer to the computed dipole

moments (1 and 15 have the highest and lowest value, respectively). The proposed identification of the isomers is given in Table 2. Experimental conditions are given in Table 1.

The solvent gradient used here is given in the Supporting Material (S4). MS-MS analyses allowed distinguishing two types of isomers: (i) KHPs with hydroperoxyl and carbonyl groups on one side of the ether function and (ii) KHPs with hydroperoxyl and carbonyl groups on both sides of the ether function. KHPs with both –OOH and –C=O groups on one side of the–O- group present a main fragment m/z 89.023 (100%) corresponding to $C_3H_5O_3$. It is followed by order of importance by m/z 71.013 ($C_3H_3O_2$) corresponding to a loss of H_2O. The presence of the fragment m/z 107.034 ($C_3H_7O_4$) was observed only when m/z 89.023 and m/z 71.013 where important (Fig. 5). $C_3H_7O_4$ can result from the loss of C_3H_5 from KHPs.

KHPs with –OOH and –C=O groups on both side of the–O- group were identified by a strong m/z 75.044 (100%) fragment, $C_3H_7O_2$, and m/z 57.033 (60%) fragment, C_3H_5O, which can result from H_2O elimination from $C_3H_7O_2$. A minor fragment at m/z 115.075 ($C_6H_{11}O_2$) which can come from –OOH elimination from KHPs was also observed.

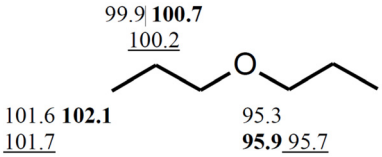

Figure 6. C–H bond dissociation energies in DPE calculated with Gaussian 09 [35] using three methods: G3B3, G3 (bold), and CBS-QB3 (underlined).

H-atom abstractions are facilitated by weaker C-H bonds near the ether function (Figure 6) already observed in kinetic studies of a series of ethers + OH reactions [36]. Nevertheless, the present results indicated that KHPs and other low-temperature oxidation products derive from reactions not limited to that of CH_2 groups in α-position to the ether function.

To further identify the isomers pertaining to the above delineated two groups of KHPs, their dipole moment was computed by different methods [35, 37] . Because of the ACN-water gradient used (from 5 to 85% ACN) the polarity of the solvent decreases over elution time. Then the more polar KHPs should be eluted first.
Taking this into consideration, a tentative identification of KHP isomers was done (Figure 5). One can see that the most probable KHP (#11) 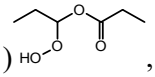

, based on C-H bond energies (Figure 6) and size of the cyclic intermediate for internal H-atom transfer, shows the largest signal, in agreement with both MS^2 data and computed dipole moments.

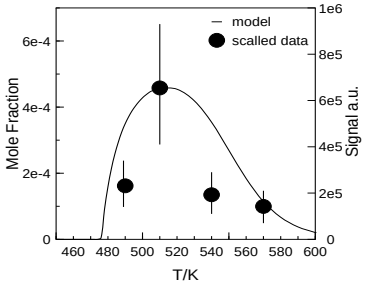

Figure 7. Comparison between experimental (symbols) and computed total mole fraction of KHPs (1000 ppm of DPE, φ = 0.5, 0.7 s, and 10 atm). The data are scaled to the computed maximum concentration. Experimental errors are estimated to be of the order of 40%.

Figure 7 shows a comparison of the experimental results and chemical kinetic modeling for the sum of KHPs. As can be seen from this figure, the chemical kinetic model well predicts the variation of KHPs concentration as a function of temperature in the cool flame regime.

Besides, 1-propanol is formed at ppm level through molecular elimination, DPE (+M) ⇆ 1-C_3H_7OH + C_3H_6 (+M), and propanal, produced via $CH_3CH_2CH(OOH)OC(=O)CH_2CH_3$ → C_2H_5CHO + $C_2H_5CO_2$ + OH (73%) and $CH_3CH_2CH(.)OCH(OOH)CH_2CH_3$ ⇆ 2 C_2H_5CHO + OH (14%) at 550 K, was measured (Fig. 2). Three cyclic ethers were also detected at m/z 117.0911 and separated by UHPLC (Supplementary Material S5). Finally, HOMs

with formula $C_6H_{12}O_8$ were also detected in flow injection analyses and negative ionization mode. Their separation by UHPLC was performed with some success but the analytical method needs to be improved.

Conclusion and Perspectives

The oxidation of di-n-propyl-ether was performed in a jet-stirred reactor at 1 and 10 atm and a constant equivalence ratio of 0.5. Residence times of 1 and 0.7 s were used at 1 and 10 atm, respectively. Mole fractions of the reactants and stable products formed during the oxidation of di-n-propyl-ether were obtained through sonic probe sampling, gas chromatography, and Fourier transform infrared spectrometry.

Hydroperoxides, ketohydroperoxides, carboxylic acids, and highly oxygenated molecules resulting from the addition of up to four O_2 on the fuel's radicals where observed using high resolution mass spectrometry analyses. Both syringe direct injection and UHPLC-HRMS were used with +/- HESI and +/-APCI. The results indicated that products derive from reactions not limited to that of CH_2 groups in α-position to the ether function. MS-MS analyses indicated the formation of two types of oxygenated products: oxygenates with hydroperoxy and keto groups located (i) on both side of the ether function, and (ii) on one side of the ether function. We attempted to further identify these isomers by using computed dipole moments, but more advanced computations are probably required to reduce uncertainties in products identification. NMR analyses of the KHP isomers should help finalizing identification. HOMs were detected but more work is needed to identify the different isomers and improve their separation by UHPLC.

Whereas our kinetic reaction mechanism represents the experimental data for most stable species and the qualitative evolution of total KHPs concentration, it needs to be expended for simulating the formation of newly detected species.

Acknowledgements

The authors gratefully acknowledge funding from the Labex Caprysses (convention ANR-11-LABX-0006-01) and through the projects PROMESTOCK and APROPOR-E (Région Centre Val de Loire, FEDER and CPER).

References

1. Yasunaga, K., et al., *A Multiple Shock Tube and Chemical Kinetic Modeling Study of Diethyl Ether Pyrolysis and Oxidation.* The Journal of Physical Chemistry A, 2010. **114**(34): p. 9098-9109.
2. Gillespie, F., et al., *Measurements of flat-flame velocities of diethyl ether in air.* Energy, 2012. **43**(1): p. 140-145.
3. Werler, M., et al., *Ignition delay times of diethyl ether measured in a high-pressure shock tube and a rapid compression machine.* Proceedings of the Combustion Institute, 2015. **35**(1): p. 259-266.
4. Vin, N., O. Herbinet, and F. Battin-Leclerc, *Diethyl ether pyrolysis study in a jet-stirred reactor.* Journal of Analytical and Applied Pyrolysis, 2016. **121**: p. 173-176.
5. Tran, L.-S., et al., *Experimental and kinetic modeling study of diethyl ether flames.* Proceedings of the Combustion Institute, 2017. **36**(1): p. 1165-1173.
6. Serinyel, Z., et al., *An experimental chemical kinetic study of the oxidation of diethyl ether in a jet-stirred reactor and comprehensive modeling.* Combustion and Flame, 2018. **193**: p. 453-462.
7. Uygun, Y., *Ignition studies of undiluted diethyl ether in a high-pressure shock tube.* Combustion and Flame, 2018. **194**: p. 396-409.
8. Tran, L.-S., et al., *Low-temperature gas-phase oxidation of diethyl ether: Fuel reactivity and fuel-specific products.* Proceedings of the Combustion Institute, 2019. **37**(1): p. 511-519.
9. Thion, S., et al., *A chemical kinetic study of the oxidation of dibutyl-ether in a jet-stirred reactor.* Combustion and Flame, 2017. **185**: p. 4-15.
10. Serinyel, Z., et al., *A high pressure oxidation study of di-n-propyl ether*, in *MCS11, 11th Mediterranean Combustion Symposium* https://hal.archives-ouvertes.fr/hal-02273272. 2019: Tenerife, Spain.
11. Perrin, O., et al., *Determination of the isomerization rate constant HOCH2CH2CH2CH(OO center dot)CH3->(HOCHCH2CH2CH)-H-center dot(OOH)CH3. Importance of intramolecular hydroperoxy isomerization in tropospheric chemistry.* Int J Chem Kinet, 1998. **30**(12): p. 875-887.
12. Blin-Simiand, N., et al., *Ketohydroperoxides and ignition delay in internal combustion engines.* Combust Flame, 1998. **112**: p. 278-282.
13. Heiss, A. and K. Sahetchian, *Isomerization reactions of the n-C4H9O and n-OOC4H8OH radicals in oxygen.* Int J Chem Kinet, 1996. **28**(7): p. 531-544.
14. Sahetchian, K., et al., *Experimental study and modeling of dodecane ignition in a diesel engine.* Combust Flame, 1995. **103**(3): p. 207-220.
15. Zinbo, M., R.K. Jensen, and S. Korcek, *Gas-liquid-chromatography of oxygenated compounds related to autoxidation of n-hexadecane.* Analytical Letters, 1977. **10**(2): p. 119-132.
16. Jensen, R.K., et al., *Liquid-phase autoxidation of organic-compounds at elevated-temperatures .1. stirred flow reactor technique and analysis of primary products from normal-hexadecane autoxidation at 120-degrees-C 180-degrees-C.* Journal of the American Chemical Society, 1979. **101**(25): p. 7574-7584.

17. Jensen, R.K., et al., *Liquid-phase autoxidation of organic-compounds at elevated-temperatures .2. Kinetics and mechanisms of the formation of cleavage products in normal-hexadecane autoxidation.* Journal of the American Chemical Society, 1981. **103**(7): p. 1742-1749.
18. Jensen, R.K., M. Zinbo, and S. Korcek, *HPLC determination of hydroperoxidic products formed in the autoxidation of normal-hexadecane at elevated-temperatures.* Journal of Chromatographic Science, 1983. **21**(9): p. 394-397.
19. Jensen, R.K., S. Korcek, and M. Zinbo, *Formation, isomerization, and cyclization reactions of hydroperoxyalkyl radicals in hexadecane autoxidation at 160-190-degrees-C.* Journal of the American Chemical Society, 1992. **114**(20): p. 7742-7748.
20. Wang, Z.D., et al., *n-Heptane cool flame chemistry: Unraveling intermediate species measured in a stirred reactor and motored engine.* Combustion and Flame, 2018. **187**: p. 199-216.
21. Wang, Z., et al., *Unraveling the structure and chemical mechanisms of highly oxygenated intermediates in oxidation of organic compounds.* Proceedings of the National Academy of Sciences, 2017. **114**(50): p. 13102-13107.
22. Bianchi, F., et al., *Highly Oxygenated Organic Molecules (HOM) from Gas-Phase Autoxidation Involving Peroxy Radicals: A Key Contributor to Atmospheric Aerosol.* Chemical Reviews, 2019. **119**(6): p. 3472-3509.
23. Dagaut, P., et al., *Ketohydroperoxides and Korcek mechanism identified during the oxidation of dipropyl ether in a JSR by high-resolution mass spectrometry*, in *MCS11 11th Mediterranean Combustion Symposium* https://hal.archives-ouvertes.fr/hal-02137413. 2019: Tenerife, Spain.
24. Dagaut, P., et al., *A Jet-Stirred Reactor for Kinetic-Studies of Homogeneous Gas-Phase Reactions at Pressures up to 10-Atmospheres (~ 1 MPa).* Journal of Physics E-Scientific Instruments, 1986. **19**(3): p. 207-209.
25. Dayma, G., C. Togbe, and P. Dagaut, *Experimental and Detailed Kinetic Modeling Study of Isoamyl Alcohol (Isopentanol) Oxidation in a Jet-Stirred Reactor at Elevated Pressure.* Energy & Fuels, 2011. **25**(11): p. 4986-4998.
26. Dagaut, P. and F. Lecomte, *Experiments and kinetic modeling study of NO-reburning by gases from biomass pyrolysis in a JSR.* Energy & Fuels, 2003. **17**(3): p. 608-613.
27. Dagaut, P., et al., *The oxidation and ignition of dimethylether from low to high temperature (500-1600 K): Experiments and kinetic modeling.* Symposium (International) on Combustion, 1998. **27**(1): p. 361-369.
28. Pasilis, S.P., V. Kertesz, and G.J. Van Berkel, *Unexpected analyte oxidation during desorption electrospray ionization-mass spectrometry.* Analytical Chemistry, 2008. **80**(4): p. 1208-1214.
29. Chen, M. and K.D. Cook, *Oxidation artifacts in the electrospray mass spectrometry of A beta peptide.* Analytical Chemistry, 2007. **79**(5): p. 2031-2036.
30. Glarborg, P., et al., *PSR: A Fortran Program for Modeling Well-Stirred Reactors, Report No. SAND86-8209, Sandia National Laboratories, Albequerque, NM*. 1986.
31. Kee, R.J., F.M. Rupley, and J.A. Miller, *CHEMKIN-II: A Fortran Chemical Kinetics Package for the Analysis of Gas-Phase Chemical Kinetics.*, in *SAND89-8009*. 1989, Sandia National Laboratories: Livermore, CA.
32. Reinnig, M.-C., J. Warnke, and T. Hoffmann, *Identification of organic hydroperoxides and hydroperoxy acids in secondary organic aerosol formed during the ozonolysis of different monoterpenes and sesquiterpenes by on-line analysis using atmospheric pressure chemical ionization ion trap mass spectrometry.* Rapid Communications in Mass Spectrometry, 2009. **23**(11): p. 1735-1741.
33. Jalan, A., et al., *New Pathways for Formation of Acids and Carbonyl Products in Low-Temperature Oxidation: The Korcek Decomposition of gamma-Ketohydroperoxides.* Journal of the American Chemical Society, 2013. **135**(30): p. 11100-11114.
34. Lide, D.R., *Handbook of Chemistry & Physics 73rd Edition*. Vol. 73. 1992, Boca Roca, FL: CRC Press. 2472.
35. Frisch, M.J., et al., *Gaussian 09*. 2009, Gaussian, Inc.: Wallingford CT.
36. Wallington, T.J., et al., *Rate Constants for the Gas-Phase Reactions of OH with C-5 through C-7 Aliphatic-Alcohols and Ethers - Predicted and Experimental Values.* International Journal of Chemical Kinetics, 1988. **20**(7): p. 541-547.
37. Gasteiger, J., and M. Marsili., *A new model for calculating atomic charges in molecules.* Tetrahedron Letters, 1978. **19**(34): p. 3181-3184.